

A Numerical Implementation of the Energy Balance Equations Based on Physical Considerations

W. Schoenmaker and R. Vankemmel

IMEC
75 Kapeldreef, B-3001 Leuven, BELGIUM

Abstract

We present an implementation of the energy balance equations in two dimensional device simulators which is based on a definite positive formulation of the ohmic energy sources for the carriers.

1. Introduction

The correct numerical treatment of the energy balance equations remains still a topic of active research. This is because naive discretizations of these equations lead to very unstable algorithms. Sometimes it may be very useful to return to the physical contents of the equations and derive a discretization prescription which is based on the underlying physics of the problem. A nice example which illustrates this statement is the Scharfetter-Gummel method for current discretization, which expresses charge conservation along a flux line segment. Starting from the physical meaning of the variables in the energy balance equations, we will derive a discretization prescription for them. Remarkably enough, we find a formulation of the energy balance equations which is well suited for considerations concerning the definiteness of the energy sources and sinks. The definite signs of these sources and sinks are very helpful in the construction of the Newton matrices, since the robustness improves considerably, if the linear solvers deal with matrices, which are semi-definite. [1] In this paper we will reformulate the energy balance equations in such a way that (1) the physical meaning of the variables is respected in the discretization procedure and (2) it becomes very straightforward to satisfy the condition that the Newton matrix is semi-definite.

2. The Hydrodynamic Model

The energy balance equations in steady state operation are (see Forghieri et al. [2])

$$\vec{\nabla} \cdot \vec{S} - \vec{E} \cdot \vec{J} + Uw + c \frac{w - w^*}{\tau_w} = 0 \quad (1)$$

where $c = p$ for holes and $c = n$ for electrons. The carrier energies are

$$w = \frac{1}{2}mv^2 + \frac{3}{2}kT \quad (2)$$

For the currents we use the thermodynamic relations

$$\vec{J} = q\mu c\vec{E} - sq\mu kT\vec{\nabla}c - sq\mu kc\vec{\nabla}T \quad (3)$$

The 'energy' flux vectors are

$$\vec{S} = -\kappa\vec{\nabla}T + \frac{s}{q}(w + kT)\vec{J} \quad (4)$$

The convective term in the energy flux vector has been neglected. This is motivated by the fact that we only take into account fluxes which are linear dependent of the driving mechanisms, \vec{E} , $\vec{\nabla}T$ and $\vec{\nabla}c$.

The vector \vec{S} can not be considered as the correct energy flux vector. This is because the *physical* energy flux vector is given by

$$\vec{S}_{phys} = -\kappa\vec{\nabla}T + \frac{s}{q}w\vec{J} \quad (5)$$

Each term has a clear physical interpretation. The first term corresponds to heat conduction, i.e. energy transport without matter transport, whereas the second term represents the energy transport due to matter transport. As a consequence, the following expression,

$$\vec{\nabla} \cdot (\vec{S} - \vec{S}_{phys}) = \frac{sk}{q}\vec{\nabla} \cdot (T\vec{J}) \quad (6)$$

must be considered as a heat source in the energy balance equation. Indeed, since $\vec{J} = sc\vec{v}$, we have

$$\vec{\nabla} \cdot (T\vec{J}) = \vec{J} \cdot \vec{\nabla}T + sT\vec{v} \cdot \vec{\nabla}c + sTc\vec{\nabla} \cdot \vec{v} \quad (7)$$

and the energy balance equations become with using $\vec{F} = \frac{\vec{J}}{\mu c}$

$$\vec{\nabla} \cdot \vec{S}_{phys} - \frac{\vec{J}}{q} \cdot \vec{F} + wU + c\frac{w - w^*}{\tau_w} + \frac{kT}{q}c\vec{\nabla} \cdot \vec{v} = 0 \quad (8)$$

The four energy sources/sinks have a straightforward physical interpretation. The first term,

$$\Sigma^{cur} = \frac{\vec{J}}{q} \cdot \vec{F} = \frac{\mu c}{q}F^2 \quad (9)$$

corresponds to the work performed by the driving force. Note that this term is *positive definite*. Any numerical implementation should respect this property. In particular, in strong inversion layers, the numerical evaluation of F^2 is much less ambiguous than the evaluation of $\vec{E} \cdot \vec{J}$. Furthermore, the quadratic appearance of this ohmic heat source term is very suitable for analysis of the signs of its contribution to the Newton-Raphson matrix. Indeed, it suffices to evaluate the signs of J_{ij} along the links.

The last term,

$$\Sigma^{com} = -\frac{kT}{q}c\vec{\nabla} \cdot \vec{v} \quad (10)$$

corresponds to a change in energy density due to a compression of the carriers.

The reformulation with Σ^{cur} is also very instructive if we consider it together with Σ^{latt} . Since $\vec{v} = s\mu\vec{F}$, we obtain

$$\Sigma^{cur} + \Sigma^{latt} = \left(1 - \frac{1}{2}\frac{m\mu}{q\tau_w}\right)\frac{\mu c}{q}F^2 - \frac{3}{2}kc\frac{T - T^*}{\tau_w} \quad (11)$$

There cannot be relaxed more kinetic energy to the lattice than the driving force can perform work, therefore we obtain the following consistency condition

$$1 - \frac{1}{2} \frac{m\mu}{q\tau_w} = 1 - \frac{1}{2} \frac{\tau_p}{\tau_w} \geq 0 \quad (12)$$

If this condition $\tau_p \leq 2\tau_w$, is not fulfilled, we will obtain carrier cooling. This phenomenon is not observed in Monte Carlo simulations. In a recent paper of Gardner [3], in which he compares the hydrodynamic model with Monte Carlo computations, this condition is indeed satisfied.

3. Scharfetter-Gummel fluxes.

The Scharfetter-Gummel method expresses the fluxes D_{ij} , J_{ij} and S_{ij} as functions of the endpoint variables: $\psi_i, c_i, T_i, \psi_j, c_j, T_j$. Since the fluxes are the linear responses to the driving mechanisms, we propose a decoupling which is based on this physical approximation, i.e. at each link of the mesh, the coefficients in front of the forces are taken constant. Then we find the following Scharfetter-Gummel fluxes for the links:

$$J_{ij}h = sq[D](c_i B(X) - c_j B(-X)) \quad (13)$$

and

$$S_{ij}h = \frac{s}{q}[\epsilon_{kin}]J_{ij}h + [\kappa](T_i B(Y) - T_j B(-Y)) \quad (14)$$

where B is the Bernoulli function. Furthermore we set $\bar{T} = (T_i + T_j)/2$ and $\Delta\psi = \psi_j - \psi_i$, etc. and

$$X = \frac{q}{k\bar{T}}s(\Delta\psi + \frac{k}{q}s\Delta T) \quad Y = -\frac{3}{2} \frac{J_{ij}h}{q[\kappa]}s \quad (15)$$

4. Applications

In order to illustrate the proposed scheme for hydrodynamical modeling we have simulated a 0.5μ gate MOSFET. The structure is depicted in Fig. 1 and corresponds to a conventional LDD. Spacers are included. The following dimensions are used: oxide thickness: 10 nm, poly thickness: 350 nm, spacer width: 250 nm, contact hole: 0.7μ , gate length: 0.5μ , silicide thickness: 50 nm, contact-spacer gap: 0.04μ , device height: 2μ .

The silicides at the source and the drain are mimiced by added a very high dopant concentration to this region such that the resistivity becomes low. The polysilicon at the gate is represented by highly doped Silicon material.

In Fig. 2 the doping concentrations for the nmos is presented, whereas Fig. 3 shows the electron temperature distribution for $|V_{DS}| = 2.5V$ and $|V_G| = 2.0V$. In Fig.4 the IV characteristics are shown for the drift-diffusion model and the hydrodynamic model.

We observe that the hydrodynamic model gives rise to lower drain currents than the drift-diffusion model. The simulations confirm the experimental observation that there are also hotspots located at the source of the transistor.

Acknowledgements. Part of this work was funded by the ESPRIT project No. 7236 ADEQUAT. Discussions with Willy Schilders (PHILIPS) and Ludo Deferm (IMEC) and An Demesmaeker (IMEC) are gratefully acknowledged.

References

- [1] W. Schilders see the proceedings SISDEP93
- [2] A. Forghieri, R. Guerrieri, P. Ciampolini, A. Gnudi, M. Rudan, G. Baccarani "A new discretization method of the semiconductor equations comprising momentum and energy balance." *IEEE Transactions on CAD Vol 7 231 (1988)*
- [3] C.L. Gardner "Hydrodynamic and Monte Carlo Simulation of an Electron Shock Wave in a One Micron Semiconductor Device" *Proceedings of the International Workshop on Computational Electronics Beckman Institute. University of Illinois at Urbana-Champaign, May 28-29, 1992*

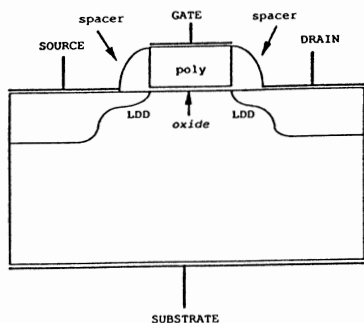


Fig.1: LDD MOS device lay-out.

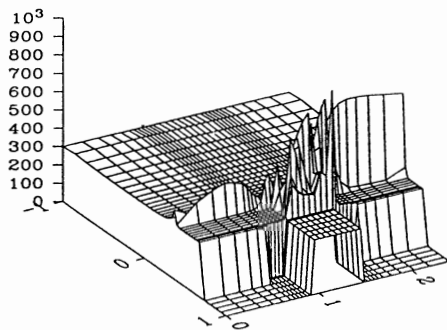


Fig.3: Electron temperature in nmos.

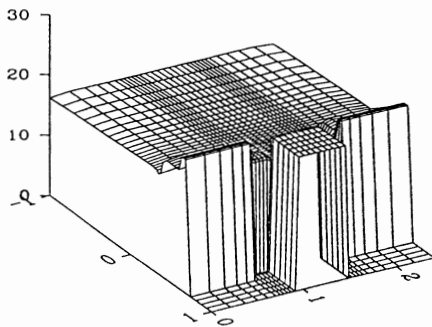


Fig.2: Log. of doping concentration.

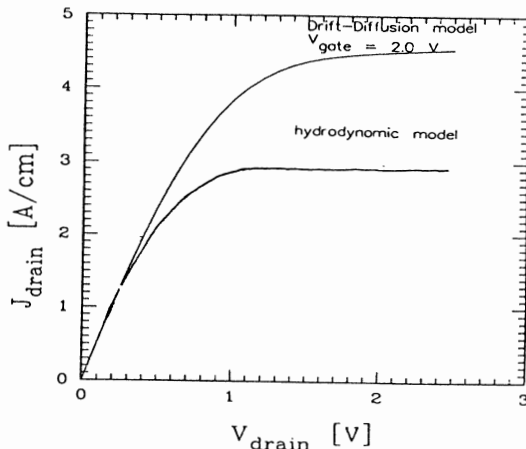


Fig.4: IV characteristic for nmos.